Structural properties of sputtered amorphous $Ga_{1-x}P_x$ films

2000 J. Phys.: Condens. Matter 12 4723

(http://iopscience.iop.org/0953-8984/12/22/305)

J. Phys.: Condens. Matter **12** (2000) 4723–4733. Printed in the UK PII: S0953-8984(00)12467-1

Structural properties of sputtered amorphous $Ga_{1-x}P_x$ films

N Elgun†, S J Gurman‡ and E A Davis‡

† Department of Physics, Faculty of Science, Ege University, Bornova, Izmir, Turkey
‡ Department of Physics and Astronomy, University of Leicester, Leicester, UK

Received 8 March 2000

Abstract. a-$Ga_{1-x}P_x$ ($0.5 \leqslant x \leqslant 1$) films have been prepared by r.f. sputtering. The local structure and bonding configurations in these films have been investigated by extended x-ray absorption fine structure (EXAFS) and infrared (IR) spectroscopy measurements. The results show that the network of the films is chemically ordered over the composition range studied. They also show that excess P atoms are incorporated with fourfold coordination into the network for $x < 0.8$. This indicates substitutional alloying, which in turn suggests the dopability of the material.

1. Introduction

Amorphous III–V semiconductors, like their crystalline counterparts, show electroluminescence effects in which visible light from green to blue is emitted [1, 2]. Such a property together with the ability to produce low-cost large-area films—the advantages of the amorphous phase—make these materials particularly promising for optoelectronic display applications. Their other properties, for example sensitivity to electron radiation and antiguide effects, are exploited in devices such as optical-image correlators [3] and vertical-cavity surface-emitting lasers (VCSELs) [4], respectively. Advances in these applications certainly require a better understanding of these materials, in particular the structural and chemical disorder which determine their physical properties.

Determination of the disorder, in particular chemical disorder as exemplified by 'wrong' bonds, has been the aim of most previous work on a-III–Vs. Direct structural methods of electron diffraction, EXAFS, IR and Raman spectroscopy, as well as non-direct methods, such as XPS, UPS, optical absorption, conductivity and ESR, have been used for thin-film samples prepared mainly by flash evaporation or sputtering. The results, in general, indicate that a-GaAs is essentially chemically ordered [5–7] whereas a-InP contains some In–In or P–P bonds [8–10], the amounts of which are somewhat less in sputtered samples than in those prepared by flash evaporation. a-InSb [8], a-AlSb [8] and a-GaSb [11] also contain small quantities of Sb–Sb bonds. For a-GaP, however, there is still controversy over the presence of wrong bonds: P–P bonds with a proportion as high as 25% were detected in flash-evaporated samples by Udron *et al* [12] whilst our structural studies by EXAFS and IR spectroscopy [13] revealed no (or very few, below the detectable limits of the techniques) wrong bonds in sputtered samples, in agreement with XPS [14] and Raman spectroscopy [8]. Nevertheless, the common belief for a-GaP is that the material contains a high number of Ga–Ga or P–P bonds. This was favoured to explain the large shrinkage of the optical gap relative to that of c-GaP and the unusual pressure and temperature dependences of the gap [15]. Interestingly, sputtered samples with high chemical ordering still show this large shrinkage in their optical gaps [16]

0953-8984/00/224723+11$30.00

and hence the present authors drew attention, in the light of the theoretical work of O'Reilly and Robertson [17], to structural disorder, mainly of the dangling-bond type, as an alternative explanation.

In order to elucidate further the wrong-bond problem in a-GaP, in the present work, P-rich a-$Ga_{1-x}P_x$ films with composition, x, in the range $0.5 \leqslant x \leqslant 1$ were investigated using EXAFS and IR spectroscopy. In these films, because of the excess P, a high number of P–P bonds occur, which can be easily detected and quantified. One should not, however, consider all the P–P bonds at off-stoichiometric compositions as 'wrong' bonds, because alloying with its own constituent element necessitates a certain fraction of like-atom bonds, and therefore the usual definition of wrong bonds for the stoichiometric composition should be modified. We define, in this paper, the wrong bonds at off-stoichiometric compositions as like-atom bonds that are in excess of the expected number of like-atom bonds in relation to the composition. Such a definition is compatible with the chemically ordered bond network (CBN) model proposed by Lucovsky *et al* [18] to specify the distribution of bonds in binary alloys. The other model, which serves the same purpose in a different way, is the random bond network (RBN) model. By comparing both models with the experimental data for a-$Ga_{1-x}P_x$ films, we unambiguously show that a-$Ga_{1-x}P_x$ is chemically ordered for a wide composition range ($0.5 \leqslant x \leqslant 1$). The present study also gives information about bonding and atomic configurations in going from stoichiometry to pure a-P.

2. Experimental procedure

The a-$Ga_{1-x}P_x$ films were prepared by r.f. sputtering carried out in an argon atmosphere at a pressure of 3–5 mTorr. As the target, a 4 in diameter stoichiometric polycrystalline GaP wafer was employed, to which small pieces of red phosphorus (99.999% pure) were increasingly added in order to vary the composition of the films systematically. During the sputtering, an r.f. power of 250 W, operating at a frequency of 13.56 MHz, was applied to the target, which resulted in a bias voltage of 680 V. The substrates were 5 cm away from the target and maintained at about 20 °C by water cooling. These conditions gave deposition rates ranging from 30 to 60 Å min^{-1}, depending on the composition.

The films were deposited on a variety of substrates: c-Si wafers were used for IR spectroscopy while Mylar sheets and Cu plates were chosen for EXAFS Ga and P K-edge experiments respectively, fused silica for reflectance measurements and Al foil for composition determinations. The thickness of the films lay between 0.85 and 1.90 μm, and was determined from an optical technique using interference fringes in reflectance spectra.

The compositions of the films were measured by energy dispersive x-ray analysis (EDAX) attached to a D.S. 130 scanning electron microscope (SEM). EDAX was also used to check the compositional uniformity across the films by taking line profiles for both Ga and P elements.

EXAFS experiments on the Ga and P K-edges were performed at the synchrotron radiation source at the SERC Daresbury Laboratory, UK. The Ga-edge x-ray absorption spectra $\mu_{Ga}(E)$ were obtained for the films in the composition range $0.5 \leqslant x < 0.98$ at the 7.1 station in the transmission mode and for the films with $x \geqslant 0.98$ (i.e. very dilute Ga content) at the same station in the fluorescence mode. The P-edge x-ray absorption spectra $\mu_P(E)$ were recorded for all the films at the 3.4 station using the electron drain-current method which is a modification of the total electron yield technique. The measured $\mu(E)$ were background subtracted using low-order polynomials with the aid of the EXBACK program to give the EXAFS function $\chi(E)$, which was then converted into $\chi(k)$ (where k is the photoelectron wavevector) and weighted by k^3 so as to compensate for the diminishing amplitudes at high k values. Short-range structural information on the films, namely coordination number, N_j,

interatomic spacing, r_j, and Debye–Waller factor, σ_j^2, for each shell, j of atoms surrounding the absorbing atom, Ga or P, were obtained by the EXCURV90 iterative analysis program. The program carries out a non-linear least-squares fitting to the experimental $k^3\chi(k)$ of the theoretical $k^3\chi(k)$ calculated according to the fast curved wave theory which takes advantage of angle-averaging appropriate for amorphous materials. The program also determined the $\pm 2\sigma$ uncertainties of the correlated structural parameters using the statistical test of Joyner *et al* [19]. A full description of the data collection and analysis procedures can be found in [13].

Infrared transmission spectra of the films were taken over the wavenumber range 4000–200 cm^{-1} ($\lambda = 2.5$–$50\ \mu m$) with a double-beam Perkin– Elmer 580 B spectrometer. During the data taking, a blank c-Si wafer was used in the path of the reference beam to eliminate the substrate effect and the sample compartment was thoroughly flushed by dry air to remove absorption by water vapour.

3. Results

3.1. EXAFS

Figure 1 shows examples of the least-squares fittings of the k^3-weighted theoretical EXAFS functions to the experimental EXAFS functions, from which the local atomic arrangements around the Ga and P atoms were determined. Figure 1 also shows the Fourier transforms (FTs) of the EXAFS functions, which were phase corrected so that the peaks corresponding to near-neighbour shells lie at the true distances. The fitting analysis revealed that the single peak in the Ga-edge FT, appearing at 2.33 Å for all the films investigated, is due to Ga–P bonds. The major peak in the P-edge FT, in contrast, was found to change position from 2.31 to 2.17 Å as the composition of the films varied from that of GaP ($x = 0.5$) to pure P ($x = 1$), indicating the presence of different contributions to the peak, which are not separated sufficiently to be resolved individually. Nevertheless, owing to differences in the phase shifts of different neighbouring atoms, the contributions were easily identified as due to P–Ga and P–P bonds. This result was obtained for the case of P-rich a-$Ga_{1-x}P_x$ films with $0.5 < x < 1$ whereas, for the cases of $x = 0.5$ and $x = 1$, solely P–Ga and P–P bonds, respectively, were found to contribute to the peak. The minor peaks in the P-edge FT were attributed to residual background and/or Fourier truncation effects.

The lengths of the bonds of Ga–P, P–Ga and P–P, which were indicated by the peak positions, are 2.33, 2.31 and 2.17 Å, respectively, independent of the composition. The former two bonds, in fact, are the same bond determined from Ga- and P-edge data, so their lengths are consistent with one another within the experimental uncertainty (±0.02 Å). The mean square deviations in these bonds lengths, represented by Debye–Waller factors, were found to be 0.013 $Å^2$ (Ga edge) and 0.012 $Å^2$ (P edge) for Ga–P bonds and 0.007 $Å^2$ for P–P bonds (all to ±0.001 $Å^2$). These values were also independent of the sample composition.

The N_{Ga-P} and N_{P-Ga} partial coordination numbers, as deduced from the fittings at the Ga and P edges, respectively, are given in figures 2 and 3 as a function of composition. The average coordination numbers expected from the CBN and RBN models calculated for a completely tetrahedral system (a 4:4 system) are also included in the figures. These models are well known and their calculation details may be found in [20]. As can be seen from the figures, the experimental data points closely follow the OBN model in both cases, which clearly shows that a-$Ga_{1-x}P_x$ films are chemically ordered not only at stoichiometry but over the entire composition range from 0.5 to 1. This means that, at each composition, the number of heteropolar Ga–P bonds is first maximized and then the remaining P atoms bond to one another

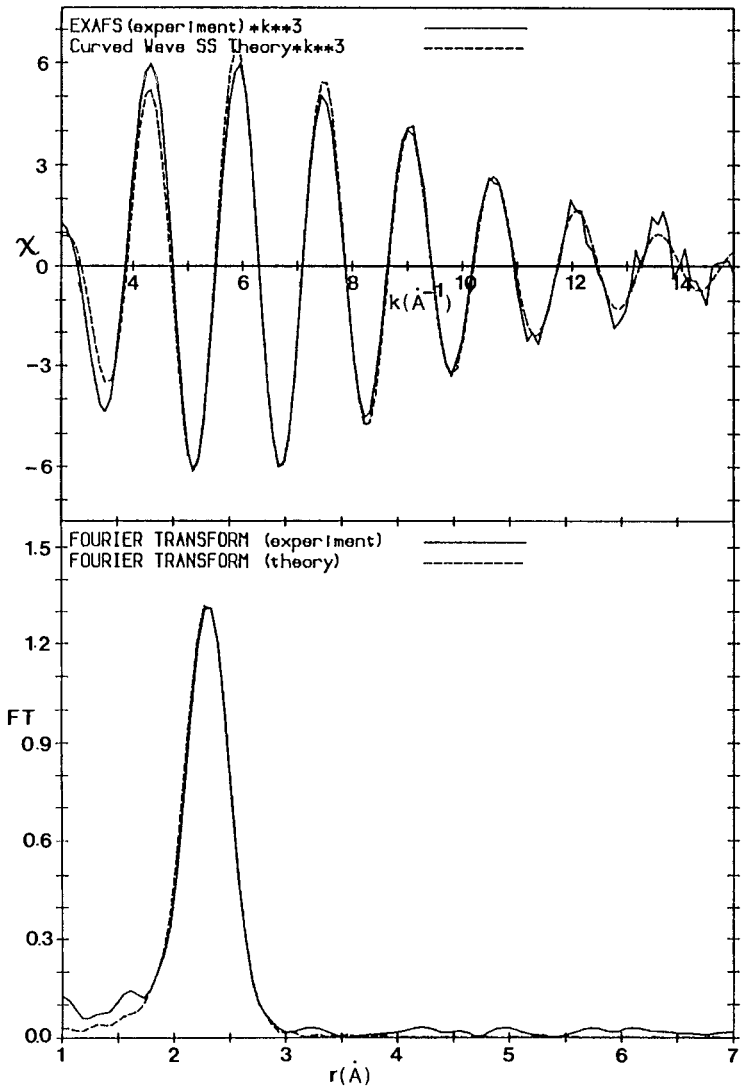

(a)

Figure 1. The k^3-weighted EXAFS function χ and Fourier transform FT for the a-$Ga_{1-x}P_x$ sample with $x = 0.72$ at (a) the Ga K edge (b) the P K edge.

to form P–P bonds. The number of P–P bonds, i.e. the N_{P-P} partial coordinations, plotted as a function of composition in figure 4, is consistent with the expected coordination number for the OBN model up to a composition of about 0.8, thus confirming chemical ordering for the films containing up to 80% P content. At higher compositions, however, the number of P–P bonds gradually deviates from the expected values towards those predicted, again from the OBN model, but for a 4:3 system, and reaches 3 when $x = 1$. The data, together with the OBN models, show that beyond $x = 0.8$ the P coordination changes gradually from fourfold to threefold, causing the network to become finally like that of a-P. The same result can also be seen more directly in figure 5 where the total P coordination, obtained by summing the N_{P-Ga} and N_{P-P} partial coordinations, is given as a function of composition. Such a change in the

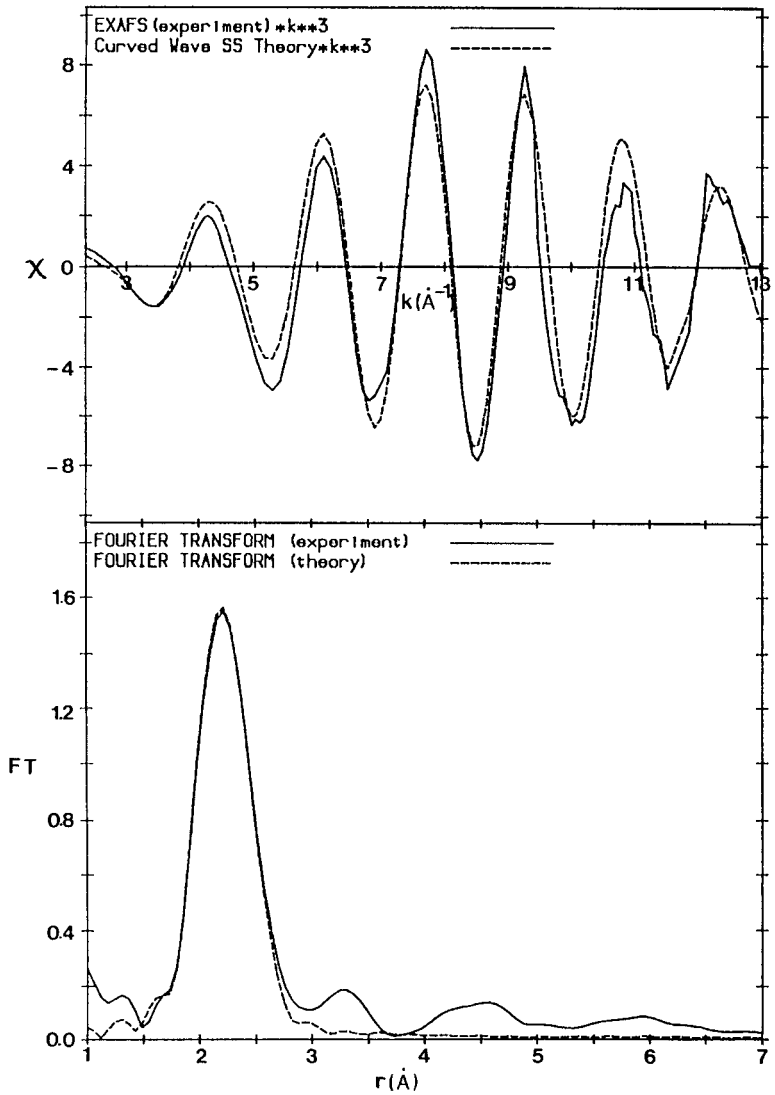

(b)

Figure 1. (Continued)

network is not, however, unexpected in view of the alloying (self-compensation) of GaP with P which, following the 8-*N* rule where *N* is the valence number, has threefold coordination. The interesting feature of figure 5 is that this change does not begin until the P content in the films is as high as 80 at.%, and before this critical P level the P atoms stay fourfold coordinated, thereby breaking the 8-*N* rule. This type of alloying is called substitutional alloying, and has not been reported so far in a-III–V materials. Its presence, however, was predicted theoretically by Robertson [21] but for a very narrow off-stoichiometric composition range of 0.49–0.51. Beyond this range self-compensated alloying was expected to take over, but our results show it occurs over a much wider range of compositions.

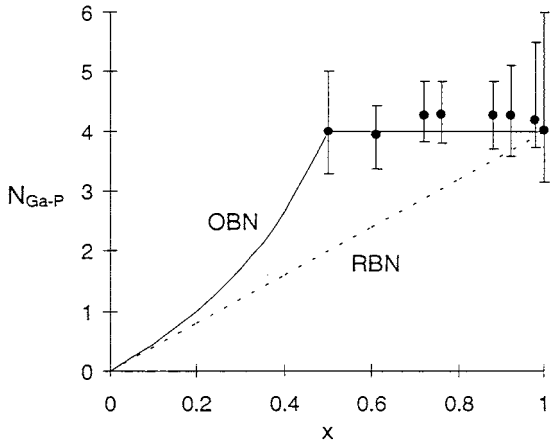

Figure 2. N_{Ga-P} partial coordination number as a function of composition. OBN model (——) and RBN model (· · · · · ·).

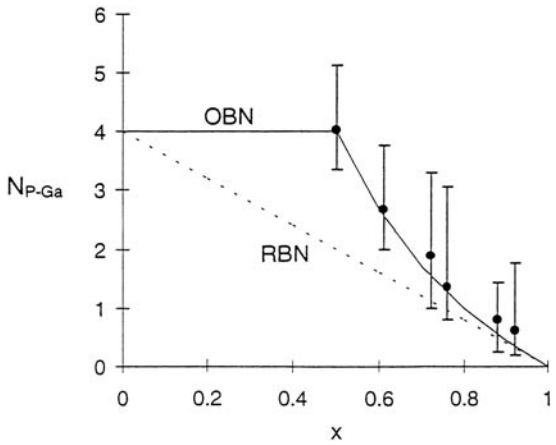

Figure 3. N_{P-Ga} partial coordination number as a function of composition. OBN model (——) and RBN model (· · · · · ·).

3.2. Infrared spectroscopy

Figure 6 shows infrared transmission spectra of the a-$Ga_{1-x}P_x$ films in the spectral range containing vibrational features. For the stoichiometric film ($x = 0.5$), the spectrum reveals two distinct bands, both of which were investigated in our previous work [13]. There the strong band located at 345 cm^{-1} was attributed to the stretching (TO) mode of the Ga–P bond, and the weak broad band around $\sim$ 590 cm^{-1} was assigned as a combination of various modes of the same bond.

The spectrum of the elemental amorphous phosphorus film ($x = 1$) also reveals two bands, well separated by a deep pseudogap at 300 cm^{-1}. The lower-lying band is centred around 270 cm^{-1} while the higher-lying one with sharp peaks at 340 and 435 cm^{-1} covers the range 300–500 cm^{-1}. Various assignments have been given for these bands in the literature depending on the possible structures to be adopted by a-P. The inelastic neutron scattering study of Gompf *et al* [22] unambiguously showed that the structure of bulk a-red P is based on

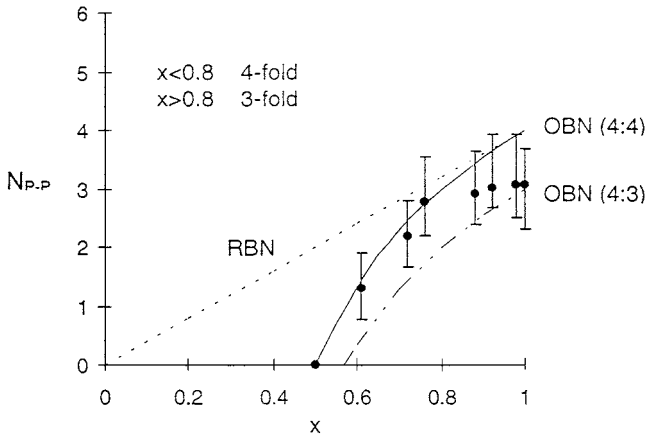

Figure 4. N_{P-P} partial coordination number as a function of composition. The theoretical values for an OBN model for a 4:4 system (——), an OBN model for a 4:3 system (— · · —) and an RBN model for a 4:4 system (· · · · · ·) are shown.

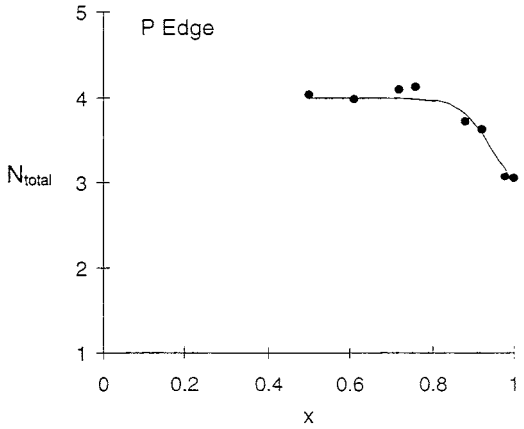

Figure 5. Total P coordination as a function of composition. The solid line is drawn as a guide to the eye.

monoclinic Hittorf's P, a crystalline allotrope of P. However, according to Olego *et al* [23], thin a-P films can have structures similar to either orthorhombic black P or to monoclinic Hittorf's P, and moreover a continuous transformation from the former structure to the latter is obtained with increasing substrate temperature. Comparison of the overall shape of the spectrum of our a-P film in figure 6 with that of the Raman spectra of a-P thin films deposited at various substrate temperatures and of bulk a-red P [23], and also with the phonon density of states of orthorhombic black and Hittorf's P [24], indicate that our film has a structure resembling more that of Hittorf's P. In particular, the existence of the sharp 340 cm^{-1} peak gives evidence for the presence of pentagonal tubes—the basic structural element of Hittorf's P—in the network of our a-P film. The pentagonal tubes, in the crystalline case, consist of cage-like P_8 and P_9 clusters connected alternately by pairs of phosphorus atoms. In our case, however, owing to the high disorder of the amorphous network, as suggested by the broadness, smoothness and the red shift (about 10–15 cm^{-1}) of our spectrum relative to that of Hittorf's P, the P_8 and

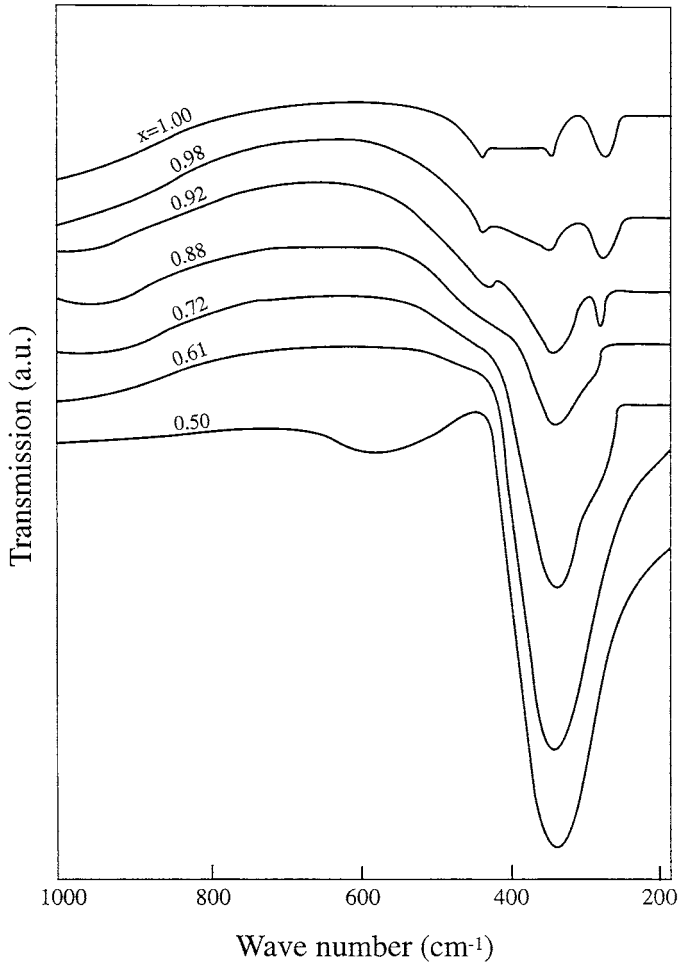

Figure 6. Infrared transmission spectra of a-$Ga_{1-x}P_x$ films. The compositions, x, label the spectra.

P_9 cages are expected to be severely distorted and broken up. Hence, the pentagonal tubes are shortened from their original length of 9.15 Å [25] and various sizes of P clusters linked to one another appear in the network. In the light of such a structure, by reference to [26], the peak at 435 cm^{-1} attributed to P–P bond-stretching vibrations that propagate along the distorted tubes, and the peak at 340 cm^{-1} could be assigned as transverse stretching of the P_8 and P_9 cages. The higher-lying band also contains localized stretching vibrations of the cage fragments and bending modes. The lower-lying band, peaking at 270 cm^{-1}, may be due to torsional vibrations of groups of P atoms as well as extended bond bendings.

For the films with compositions between 0.5 and 1, the spectra in figure 6 show systematic changes in the vibrational bands, indicating a continuous transformation of the a-GaP network to that of a-P. The first change to be noted, on going from stoichiometry to the elemental P, is a rapid reduction in intensity of the strong band associated with the stretching mode of the Ga–P bonds. This reduction, together with the disappearance of the smaller band related also to Ga–P bonds, indicate the expected decrease in the number of Ga–P bonds in the network of the films. At the same time, P–P bonds begin to form, which show themselves first as a

very shallow broad band with a midpoint of ~ 490 cm^{-1} in the spectrum of the a-$Ga_{0.39}P_{0.61}$ sample. This band then deepens, and its midpoint peaks and shifts to 435 cm^{-1} with increasing P content. The P–P bonds also give rise to a shoulder attached to the strong band on the lower-wavenumber side (~ 300 cm^{-1}) when the P composition is raised to 0.72. As the composition is further raised, the shoulder shifts towards lower wavenumbers and finally separates from the band, forming the lower-lying band centred around 270 cm^{-1}. In addition to the above bands, there is one more P–P bond-related band (~ 340 cm^{-1}), which, however, cannot be seen until the P composition is 0.99, because it occurs too close to the Ga–P bond-related strong band (345 cm^{-1}) and also is affected by the presence of the lower-lying band.

The evolution of the IR bands and the shift in their wavenumbers by as much as 55 cm^{-1} (from 490 to 435 cm^{-1}) indicate major changes in the phosphorus environment followed by the progressive dilution of Ga in P. For the films with compositions closer to stoichiometry, the wavenumbers at which the shoulder and very shallow broad band occur (300 and 490 cm^{-1}, respectively) agree surprisingly well with the theoretical wavenumbers (300 and 500 cm^{-1}) calculated for fourfold coordinated defects in a fully threefold pyramidal structure of a-P [27]. As for the films with compositions closer to the pure P side, the wavenumbers of the observed bands are consistent with the theoretical wavenumbers calculated for threefold coordinated P atoms forming the P_8 and P_9 cages in Hittorf's P [26]. These findings thus support fourfold coordination of P atoms in the films with $x < 0.8$, and threefold coordination of P atoms in the films with $x > 0.8$, confirming the result obtained from the EXAFS experiments.

Apart from the change in the short-range order around P atoms, the evolution of the vibrational bands of the films, in particular that of the extremely P-rich films, also reveal the creation and development of intermediate-range order. The formation of the cage-like P_8 and P_9 clusters or cluster fragments show that the network order is extended to about 4–5 Å, i.e. the size of the cages [26]. Further extension occurs when the clusters link to each other to build the distorted tubes.

4. Discussion

So far, in the search for chemical disorder in a-GaP, samples with a composition as close to stoichiometry ($x = 0.5$) as possible were used to find out whether wrong bonds are an intrinsic property of this material. The experimental techniques were often operated at their limits of sensitivity and hence it was hard enough to detect the presence of a few per cent of wrong bonds, let alone identify their type and distribution in the network. In this work, in contrast to the previous studies, we began to survey the chemical disorder from the off-stoichiometric samples and then extrapolated the results back to the stoichiometric composition to obtain the intrinsic properties.

The EXAFS data presented in figures 2–4 reveal that the numbers of the P–Ga and P–P bonds forming the networks of the P-rich samples are in accord with the chemically ordered bond model over the entire composition range $0.61 \leqslant x \leqslant 1$, regardless of whether the network is a 4:4 or 4:3 coordinated system. Extension of this general trend to $x = 0.5$ indicates that the stoichiometric sample is also intrinsically chemically ordered and hence should not contain any P–P bonds. Nevertheless, like that of flash-evaporated a-GaP films [12], a small number of P–P bonds may occur in our stoichiometric film as a result of 'extrinsic effects' arising from strongly out-of-equilibrium conditions occurring during the deposition of the films. In such cases, from the extrapolation of N_{P-P} in figure 4, we find that the P–P bonds should maintain fourfold coordination, in contrast to all expectations for threefold coordination. According to the bond-length results, the lengths of tetracoordinated P–P bonds are 2.17 Å. The incorporation of such antisite units into a network consisting entirely of 7–10% longer Ga–P bonds causes local

stresses which may be released by breaking the host bonds, thereby creating more dangling bonds in addition to the dangling bond produced during the deposition of the films. This could explain the intrinsically high number of dangling-bond defects in the nearly stoichiometric GaP films [16].

For the off-stoichiometric samples, the atomic configuration of the extrinsic wrong (P–P) bonds cannot be distinguished from that of the expected P–P bonds. Nevertheless, figure 4 shows their sites must be fourfold coordinated on average for $x < 0.8$ so that the network coordination of four is unaltered and partially threefold at compositions $x > 0.8$. The P–P bonds in the P-rich samples also cause stresses resulting from the coexistence of two different bond lengths in the same network. This time, the stresses cannot be released by the production of extra dangling bonds owing to the network continuity; instead the formation of rings and chains through P–P linkages, as evidenced by the IR results presented in the preceding section, seems to relax the network. This relaxing mechanism is also compatible with the polymeric nature of P bonds.

The observation of substitutional alloying in the a-$Ga_{1-x}P_x$ films is a very important result since it indicates that the material can be doped. The doping mechanism is, however, expected to be different from that of a-Si:H in that the impurity atoms, usually P or B, replacing Si atoms give rise to an electron or a hole, respectively, which move freely in the conduction or valence band. As for the doping of a-GaP with P, so-called self-doping, the substitution of tetracoordinated Ga atoms by P causes an increase in the number valence electrons from eight to ten. Subsequent formation of a P–P bond, which uses up eight electrons, leaves the remaining two free to go to the conduction band. Thus, twice the number of carriers is released per substituted atom. One may speculate whether both electrons contribute to the conductivity or are trapped possibly causing interesting phenomena.

The doping of a-$Ga_{1-x}P_x$ if it is proved experimentally by electrical measurements, may result in many new technological applications. In addition to the low cost and the ability to produce large-area devices, the possibility of the occurrence of the doping in such a wide composition range, $0.5 \leqslant x < 0.8$, could be an important experimental advantage in applications since slight variations in the compositions of the samples, which might arise from a lack in control of the deposition conditions, would not affect the dopability.

Acknowledgment

One of the authors (NE) would like to thank the British Council for providing financial support during her visit to the UK.

References

[1] Kubota H and Onuki M 1989 *J. Non-Cryst. Solids* **115** 39
[2] Kubota H, Matsumoto T, Hirayu T, Fujiyoshi T, Miyagawa R, Miyahara K and Onuki M 1994 *Solar Energy Mater. Solar Cells* **35** 353
[3] Aronov D A, Isaev K I, Rubinov V M and Tuichiev M 1994 *Semiconductors* **28** 105
[4] Yoo B S, Chu H Y, Park M S, Park H H and Lee E H 1996 *Electron. Lett.* **32** 116
[5] Theye M L, Gheorghiu A and Launois H 1980 *J. Phys. C: Solid State Phys.* **13** 6569
[6] Gheorghiu A and Theye M L 1981 *Phil. Mag.* B **44** 285
[7] Baker S H, Manssor M I, Gurman S J, Bayliss S C and Davis E A 1992 *J. Non-Cryst. Solids* **144** 63
[8] Wihl M, Cardona M and Tauc J 1972 *J. Non-Cryst. Solids* **8–10** 172
[9] Udron D, Flank A M, Lagarde P, Raoux D and Theye M L 1992 *J. Non-Cryst. Solids* **150** 361
[10] Baker S H, Bayliss S C, Gurman S J, Elgun N, Williams B T and Davis E A 1994 *J. Non-Cryst. Solids* **169** 111
[11] Theye M L and Gheorghiu A 1982 *Solar Energy Mater.* **8** 331
[12] Udron D, Flank A M, Gheorghiu A, Lagarde P and Theye M P 1989 *Physica* B **158** 625

[13] Elgun N, Gurman S J and Davis E A 1992 *J. Phys.: Condens. Matter* **4** 7759
[14] Shevchik N J, Tejeda J and Cardona M 1974 *Phys. Rev.* B **9** 2627
[15] Connell G A N and Paul W 1972 *J. Non-Cryst. Solids* **8–10** 215
[16] Elgun N and Davis E A 1994 *J. Phys.: Condens. Matter* **6** 779
[17] O'Reilly E P and Robertson J 1986 *Phys. Rev.* B **34** 8684
[18] Lucovsky G, Galeener F L, Geils R H and Keezer R C 1977 *The Structure of Non-Crystalline Materials* ed P H Gaskell (London: Taylor and Francis) p 127
[19] Joyner R W, Martin K J and Meechan P 1987 *J. Phys. C: Solid State Phys.* **20** 4005
[20] Elliott S R 1990 *Physics of Amorphous Materials* (London: Longman) p 116
[21] Robertson J 1981 *Phil. Mag.* **44** 239
[22] Gompf F, Fasol G, Hönle W and Suck J B *Proc. 2nd Int. Conf. on Phonon Physics (Budapest, 1985)* ed J Kollar, N Kroo, N Menyhard and T Siklos (Singapore: World Scientific)
[23] Olego D J, Baumann J A and Schachter R 1985 *Solid State Commun.* **53** 905
[24] Hohl D and Jones R O 1992 *Phys. Rev.* B **45** 8995
[25] Olego D J 1985 *Phys. Rev.* B **31** 2230
[26] Fasol G, Cardona M, Hönle W and von Schnering H G 1984 *Solid State Commun.* **52** 307
[27] Pollard W B and Joannopoulos J D 1980 *Phys. Rev.* B **21** 760